Acta Crystallographica Section D
Biological Crystallography
ISSN 0907-4449

Crystallization and preliminary X-ray analysis of the atrial natriuretic peptide (ANP) receptor extracellular domain complex with ANP: use of ammonium sulfate as the cryosalt

Haruo Ogawa,[a] Xiaolun Zhang,[a] Yue Qiu,[a] Craig M. Ogata[b] and Kunio S. Misono[a]*

[a]Department of Molecular Cardiology, Lerner Research Institute, Cleveland Clinic Foundation, 9500 Euclid Avenue, Cleveland, OH 44195, USA, and [b]Argonne National Laboratory, 9700 South Cass Avenue, Argonne, IL 60439, USA

Correspondence e-mail: misonok@ccf.org

Received 18 June 2003
Accepted 25 July 2003

Atrial natriuretic peptide (ANP) plays a major role in blood pressure and volume regulation owing to its natriuretic and vasodilatory activities. The ANP receptor is a single-span transmembrane receptor coupled to its intrinsic guanylyl cyclase activity. The extracellular hormone-binding domain of rat ANP receptor (ANPR) was overexpressed by permanent transfection in CHO cells and purified. ANPR complexed with ANP was crystallized at 301 K by the hanging-drop vapor-diffusion method. The crystals were frozen in 3.4 *M* ammonium sulfate used as a cryoprotectant. The crystals diffracted to 3.1 Å resolution using synchrotron radiation and belonged to the hexagonal space group $P6_1$, with unit-cell parameters $a = b = 100.3$, $c = 258.6$ Å.

1. Introduction

Atrial natriuretic peptide (ANP) is a peptide hormone secreted by the heart in response to blood-volume expansion. ANP stimulates salt excretion (de Bold *et al.*, 1981) and dilates blood vessels (Currie *et al.*, 1983; Grammer *et al.*, 1983), thereby lowering the blood pressure and volume. Thus, ANP plays a central role in regulation of the cardiovascular system. Aberrations in ANP action may lead to hypertension, congestive heart failure and other cardiovascular diseases (Oliver *et al.*, 1997). The hormonal actions of ANP are mediated by a single-span transmembrane receptor coupled to its intrinsic guanylate cyclase (GCase) catalytic activity. The ANP receptor occurs as a dimer of a transmembrane polypeptide that contains a hormone-binding extracellular domain, a transmembrane domain and an intracellular domain consisting of an ATP-binding regulatory domain and the effector-enzyme GCase catalytic domain (Chinkers & Garbers, 1989). The mechanism by which binding of ANP to the extracellular domain stimulates GCase catalysis is not known.

The ANP receptor belongs to the family of membrane-bound GCase-coupled receptors that have a similar overall molecular topology and possibly share a common signaling mechanism. However, the mechanism of signaling by the ANP receptor and other GCase-coupled receptors remains largely unknown. To understand the signaling mechanism, structural studies using X-ray crystallography are essential. Previously, we overexpressed the extracellular hormone-binding domain of the ANP receptor (ANPR) in COS cells and purified it by ANP-affinity chromatography (Misono *et al.*, 1999). We crystallized ANPR without ligand (apoANPR) in its dimeric form and determined its crystal structure at 2.0 Å resolution (van den Akker *et al.*, 2000). In this study, we aim to determine the crystal structure of ANPR in complex with the hormone ANP. The structure of the complex, when compared with the apoANPR structure, will reveal the structural basis for signal transduction by the ANP receptor.

2. Materials and methods

2.1. Expression and purification of ANPR

ANPR, consisting of residues 1–435 of rat ANP receptor, was expressed by a slight modification of the previously described method (Misono *et al.*, 1999). CHO cells were transfected with pcDNA3-NPRA and stably transfected high-producing cells were cloned by selection with G-418. The cloned cells were cultured in roller bottles and the conditioned medium containing the expressed ANPR was collected every 2 d. The ANPR was purified by ANP-affinity chromatography as described in Misono *et al.* (1999).

2.2. Removal of terminal sialic acid residues by sialidase treatment

The ANPR obtained was N-glycosylated (Miyagi *et al.*, 2000). Isoelectric focusing of an ANPR preparation on a polyacrylamide gel (Invitrogen) gave several bands, apparently reflecting heterogeneity in the glycosyl structure. The multiple isoelectric points observed may arise from variations in the terminal sialic acid residues. To minimize the heterogeneity, the ANPR (100 µg) was treated with 1 mU of sialidase I (from *Clostridium perfringens*; Glyko Inc., Rosedale, NY, USA) in 50 µl of

50 m*M* Tris–HCl buffer pH 6.8 at 310 K for 12 h. After sialidase digestion, the ANPR bands on the isoelectric focusing gel converged into one major band and one minor band. The sialidase-treated ANPR was again purified by ANP-affinity chromatography.

2.3. Crystallization of the ANPR complexed with ANP

Native ANP is a 28-residue peptide with the sequence Ser-Leu-Arg-Arg-Ser-Ser-Cys-Phe-Gly-Gly-Arg-Ile-Asp-Arg-Ile-Gly-Ala-Gln-Ser-Gly-Leu-Gly-Cys-Asn-Ser-Phe-Arg-Tyr and contains an intramolecular disulfide bond between Cys7 and Cys23. To minimize the flexibility of the bound structure, we used a truncated ANP peptide consisting of residues 7–27 [ANP(7–27)] which is fully biologically active (Misono *et al.*, 1984). To form an ANP-bound complex, ANPR (1 mg ml^{-1}) in 5 m*M* HEPES buffer pH 7.0 containing 20 m*M* NaCl was incubated with a 1.1-fold excess of ANP(7–27) at room temperature for 1 h. The mixture was then concentrated using an Ultrafree centrifugal filter tube (10 kDa cutoff; Millipore) to a final ANPR concentration of 10 mg ml^{-1}. Initial trials for crystallization conditions were set up using commercially available screening kits from Hampton Research by the hanging-drop vapor-diffusion method at 277 and 293 K. Crystals were seen after several months in crystallization drops prepared by mixing 1 µl of the ANPR–ANP complex solution and 1 µl of reservoir solution consisting of 0.1 *M* Tris–HCl buffer pH 8.5 and 2.0 *M* ammonium sulfate. The conditions were optimized by varying the pH, ammonium sulfate concentration and temperature. The crystals used in this study were grown from 2.0 *M* ammonium sulfate in 0.1 *M* MES buffer pH 6.5 containing 10 m*M* NaCl at 301 K.

2.4. X-ray crystallographic studies

A high concentration of ammonium sulfate (3.4 *M*) was used as a cryoprotectant. Briefly, crystals were dialyzed against increasing concentrations of ammonium sulfate (2.2–3.4 *M* ammonium sulfate stepwise at 30 min intervals) in 0.1 *M* MES buffer pH 6.5 containing 10 m*M* NaCl. Crystals were then frozen in liquid propane. Frozen crystals were screened at 100 K using an in-house X-ray facility (Rigaku RU-200 rotating-anode X-ray generator operated at 50 kV and 100 mA with an R-AXIS IIC imaging-plate detector). Complete data sets were collected at 100 K at the National Synchrotron Light Source beamlines X4A and X25. Data were processed and scaled using *DENZO* and *SCALEPACK* (Otwinowski & Minor, 1997). Molecular-replacement trials were carried out using *CNS* (Brünger *et al.*, 1998) with the monomer structure of apoANPR (PDB code 1dp4; van den Akker *et al.*, 2000) as the search model.

3. Results and discussion

The ANPR was expressed in CHO cells permanently transfected and cloned by selection with G-418. Compared with the transient expression in COS cells used previously (Misono *et al.*, 1999), maintenance of the cells and production of the ANPR was more reliable and gave higher yields. Generally, 0.5 mg of purified ANPR could be obtained from 1 l of conditioned culture medium. X-ray diffraction by our preliminary crystals was found to be relatively weak. It was necessary to grow larger crystals to obtain higher resolution data. We showed previously that ANPR is N-glycosylated at five aspargine sites and contains considerable microheterogeneity (Miyagi *et al.*, 2000). To reduce the heterogeneity, we treated the ANPR with sialidase to remove terminal sialic acid residues. The product was then purified again by ANP-affinity chromatography. Isoelectric focusing showed that several protein bands found with the untreated ANPR converged to a single major band after the treatment. This sialidase-treatment step was effective in obtaining larger crystals. The sialidase-treated ANPR gave crystals with average dimensions of approximately 0.25 × 0.7 × 0.1 mm (Fig. 1), which were 1.5–2 times larger on average than those obtained from the untreated ANPR.

Because of the large crystal size, selection of cryoconditions was most critical. Typical cryoprotectants such as glycerol, ethylene glycol, sugars and PEG were not effective. Various cryosalts described by Rubinson *et al.* (2000) such as Li_2SO_4, $MgSO_4$ and LiCl were also tested but were not effective. We then reasoned that because our crystals were grown from a relatively high concentration of ammonium sulfate (2.0 *M*), a high concentration of the same salt could simply be used as an effective cryoprotectant. The principle of cryoprotection by a high concentration of ammonium sulfate is similar to that by cryosalts described by Rubinson *et al.* (2000). For freezing, we tested flash-cooling in a stream of nitrogen gas (100 K) and freezing using liquid nitrogen. However, these procedures caused high mosaicity in the crystal. We found that freezing in liquid propane was effective in maintaining the crystal integrity. Appar-

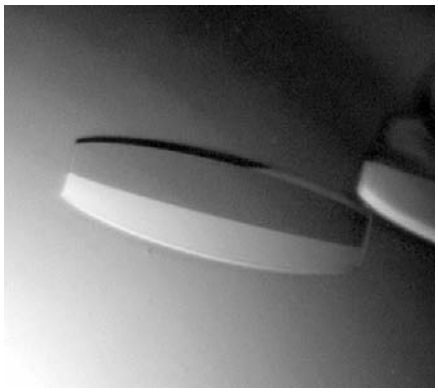

Figure 1
Crystals of ANPR complexed with ANP. The approximate size of the crystal is 0.25 × 0.7 × 0.1 mm.

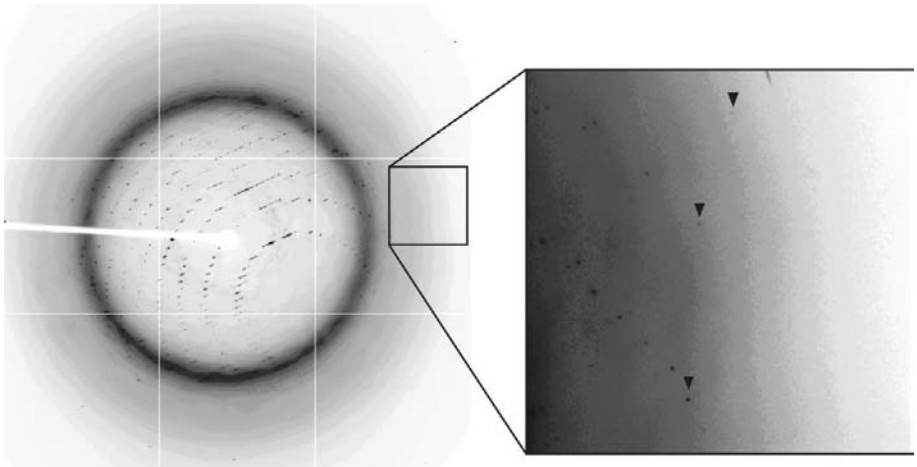

Figure 2
X-ray diffraction pattern from a crystal of the ANPR–ANP complex. The arrowheads highlight the reflection spots, from the center to the outside, at 3.00, 2.91 and 2.72 Å resolution.

ently, more rapid freezing by liquid propane was critical because of the large crystal size.

Diffraction by the ANPR–ANP complex crystal was highly anisotropic. Reflections were observed in the best direction to 2.7 Å resolution, but to only 3.4 Å resolution in the perpendicular direction (Fig. 2). Analysis of the diffraction pattern showed that the crystal belonged to the primitive hexagonal space group $P6_1$ or $P6_5$, with unit-cell parameters $a = b = 100.3$, $c = 258.6$ Å. The asymmetric unit contained two protein molecules. Based on the molecular weight of the ANPR of 48 374 Da (polypeptide residues 1–435), V_M was estimated to be 3.9 Å^3 Da^{-1} with a solvent content of 68.3% (Matthews, 1968). The V_M of our crystals was slightly higher than the general values (1.7–3.5 Å^3 Da^{-1}; Matthews, 1968). The presence of two molecules in the asymmetric unit is consistent with the finding that the ANP receptor functions as a dimer. The data-collection statistics are shown in Table 1. The R_{merge} value was relatively high, apparently owing to the anisotropy in diffraction. The overall completeness and R_{merge} were sufficient for solution of the structure by molecular replacement.

It has been reported that diffraction resolution can be improved by crystal dehydration by agents such as low-molecular-weight PEGs, glycerol and salts at high concentrations (Heras *et al.*, 2003). Our crystals were grown from 2.0 *M* ammonium sulfate. The crystals were then frozen in 3.4 *M* ammonium sulfate for data collection. In this study, we did not find an appreciable improvement in the diffraction resolution of frozen crystals (in 3.4 *M* ammonium sulfate) over that of unfrozen crystals (in 2.0 *M* ammonium sulfate), presumably because the initial crystals were already at a relatively high salt concentration.

Molecular-replacement calculations were performed using *CNS* (Brünger *et al.*, 1998) using the structure of apoANPR as the search model. We also performed molecular-replacement calculations using each of the two domains in the ANPR, the membrane-proximal domain and membrane-distal domain, individually as the search model. Essentially identical structures were obtained with the three different search models. The exact space group was identified as $P6_1$ during the initial molecular-replacement calculations. This solution gave molecules packing without any serious overlaps. The initial *R* factor was 0.374. The density for the bound ANP molecule was found between two ANPR monomers (Fig. 3), confirming the selection of the space group and the solution of the molecular-replacement calculation.

Model building and structure refinement are currently in progress. The structure will reveal binding interactions between the receptor and the hormone. Additionally, structural comparison with apoANPR is expected to uncover the structural mechanism of ANP receptor signaling.

Table 1
Data-collection statistics.

Values in parentheses are for the outermost resolution shell.

Space group	$P6_1$
Unit-cell parameters (Å)	$a = b = 100.3$, $c = 258.6$
Resolution range (Å)	25.0–3.1 (3.19–3.10)
Completeness (%)	96.15 (91.5)
Unique reflections	26639
Redundancy	14.3
R_{merge} (%)	7.1 (48.7)
$I/\sigma(I)$	35.0 (5.8)

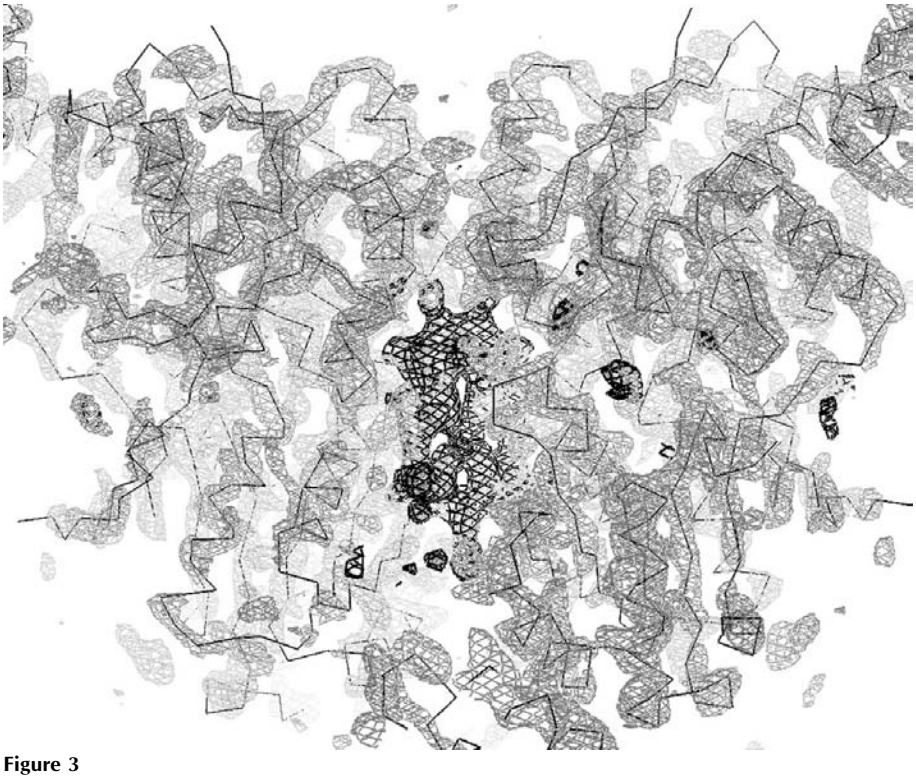

Figure 3
Initial electron-density map obtained by molecular replacement. The grey and black densities represent $2F_o - F_c$ and $F_o - F_c$ maps, respectively.

We thank Dr M. Becker for help in data collection, and Drs M. Shoham and M. Weiss for the use of their laboratory X-ray facility. This work was supported by National Institutes of Health Grant HL54329 and American Heart Association National Center Grant 95012310N to KSM. HO is a recipient of American Heart Association Ohio Valley Affiliate Postdoctoral Fellowship 0325241B.

References

Akker, F. van den, Zhang, X., Miyagi, M., Huo, X., Misono, K. S. & Yee, V. C. (2000). *Nature (London)*, **406**, 101–104.
Bold, A. J. de, Borenstein, H. B., Veress, A. T. & Sonnenberg, H. (1981). *Life Sci.* **28**, 89–94.
Brünger, A. T., Adams, P. D., Clore, G. M., DeLano, W. L., Gros, P., Grosse-Kunstleve, R. W., Jiang, J.-S., Kuszewski, J., Nilges, M., Pannu, N. S., Read, R. J., Rice, L. M., Simonson, T. & Warren, G. L. (1998). *Acta Cryst.* D**54**, 905–921.
Chinkers, M. & Garbers, D. L. (1989). *Science*, **245**, 1392–1394.
Currie, M. G., Geller, D. M., Cole, B. R., Boylan, J. G., YuSheng, W., Holmberg, S. W. & Needleman, P. (1983). *Science*, **221**, 71–73.
Grammer, R. T., Fukumi, H., Inagami, T. & Misono, K. S. (1983). *Biochem. Biophys. Res. Commun.* **116**, 696–703.
Heras, B., Edeling, M. A., Byriel, K. A., Jones, A., Raina, S. & Martin, J. L. (2003). *Structure*, **11**, 139–145.
Matthews, B. W. (1968). *J. Mol. Biol.* **33**, 491–497.
Misono, K. S., Grammer, R. T., Fukumi, H. & Inagami, T. (1984). *Biochem. Biophys. Res. Commun.* **123**, 444–451.
Misono, K. S., Sivasubramanian, N., Berkner, K. & Zhang, X. (1999). *Biochemistry*, **38**, 516–523.
Miyagi, M., Zhang, X. & Misono, K. S. (2000). *Eur. J. Biochem.* **267**, 5758–5768.
Oliver, P. M., Fox, J. E., Kim, R., Rockman, H. A., Kim, H. S., Reddick, R. L., Pandey, K. N., Milgram, S. L., Smithies, O. & Maeda, N. (1997). *Proc. Natl Acad. Sci. USA*, **94**, 14730–14735.
Otwinowski, Z. & Minor, W. (1997). *Methods Enzymol.* **276**, 307–326.
Rubinson, K. A., Ladner, J. E., Tordova, M. & Gilliland, G. L. (2000). *Acta Cryst.* D**56**, 996–1001.